

Efficient method for the calculation of rate constants for reactions with unimolecular steps

A. Koksharov^{1*}, C. Yu¹, V. Bykov¹, U. Maas¹

M. Pfeifle², M. Olzmann²

¹Institute of Technical Thermodynamics, Karlsruhe Institute of Technology, Germany

²Institute of Physical Chemistry, Karlsruhe Institute of Technology, Germany

Abstract

Rate constants of elementary reactions involving unimolecular steps can be calculated in a most general way from molecular data by solving appropriate master equations. The conventional numerical solution requires rather a fine discretization applied over a sufficiently large energy range to achieve a reasonable accuracy. This leads to linear but very high dimensional systems of differential equations. We propose a quasi-spectral method that uses the smoothness and special shape of the solution to reduce the dimensionality of the linear model. The method is based on the transformation of the solution into the space of Gaussian radial basis functions. The combination with the variable discretization scheme proposed earlier provides further advantages. The suggested approach is illustrated for the unimolecular decomposition of an intermediate radical occurring in the pyrolysis/oxidation of 2,5-dimethylfuran. A comparison of the original and the method proposed here is presented to validate the novel approach and to demonstrate its performance.

Introduction

The calculation of rate constants plays a central role for the modeling of mechanisms of chemical reactions. Rate constants can exhibit a complicated dependence on system parameters such as pressure and temperature. Furthermore, many reactions between large polyatomic compounds involve both unimolecular reversible isomerisation and decomposition.

Rate constants for such reactions can be calculated from molecular data by solving so called master equations (ME). A ME describes the time-dependent population evolution of a chemical species over its rovibrational energy levels taking into consideration chemical reactions and molecular excitation and deactivation due to collisional energy transfer in the presence of the bath gas [1–4].

All of the known analytic solutions are only valid under certain conditions (e.g. low pressure limit [3]). Commonly used numerical methods require rather a fine discretization ($\Delta E = 10 \text{ cm}^{-1}$) applied over a sufficiently large energy range (e.g. $E_{max} = 50000 \text{ cm}^{-1}$) to achieve a reasonable accuracy, leading to a linear but very high dimensional system. Furthermore, the understanding of processes of coupled elementary reactions require the solution systems of master equations which considerably increases the computational costs (see e.g. [5, 6]). Thus methods of dimension reduction are necessary. One way of model reduction is to restrict the maximum energy level that is relevant for quasi-stationary population evolution, the other way is to use a variable discretisation scheme [7].

In the current work a quasi-spectral method (QSM) is proposed that exploits the smoothness and the special shape of the solution. The method is based on the transformation of the solution into the space of Gaussian radial basis functions (GRBFs).

The suggested approach is illustrated by the unimolecular decomposition of 25DMF2H, a radical produced by H addition to the carbon in α position to the oxygen atom in 2,5-dimethylfuran (25DMF). The intermediate radical 25DMF2H can either decompose back to 25DMF + H or undergo a C-C bond scission to form a methyl radical and 2-methylfuran. The comparison of the conventional discretization method (CDM) and the proposed QSM is presented to demonstrate the performance of the suggested approach.

Mathematical Methods

Unimolecular reactions can be described by the following integro-differential equation, see e.g. [1–3]:

$$\frac{\partial n(E, t)}{\partial t} = \omega \cdot \left[\int_0^{+\infty} P(E, E') \cdot n(E', t) dE' - n(E, t) \right] - k_{\Sigma}(E) \cdot n(E, t) + R_a \cdot f(E) \quad (1)$$

with

$$k_{\Sigma}(E) = \sum_{l=1}^R k_l(E) \quad (2)$$

Here, $n(E, t)$ is the energy- and time-dependent population of the considered reactant, $\frac{\partial}{\partial t} n(E, t)$ is the change of the population over the time, ω is the collision frequency with collision partner molecules (bath gas molecules), R is the number of unimolecular reaction channels, $k_l(E)$ is the energy-specific rate constant of the l -th reaction, R_a is the rate of a formation reaction and $f(E)$ is the normalized distribution of incoming flux of the considered reactant. For a thermal activation reaction, $R_a = 0$. For a chemically activated process, R_a is normally considered as

*Corresponding author: koksharov@kit.edu

a constant, due to its significantly slower change compared to the studied process.

$P(E, E')$ is the collisional energy transfer function describing the probability of collision-induced transitions from an initial energy in the range $[E', E' + dE]$ to a final energy within $[E, E + dE]$. $P(E, E')$ must follow the principle of completeness [1]:

$$\int_0^{+\infty} P(E, E') dE = 1 \quad (3)$$

and the principle of detailed balancing [1]:

$$\frac{P(E, E')}{P(E', E)} = \frac{n^e(E)}{n^e(E')} \quad (4)$$

where n^e denotes the equilibrium distribution. To derive a discrete form of the CME, the continuous function $n(E, t)$ can be written in piecewise constant form [7]

$$n(E, t) \approx \sum_{i=1}^N n_i(t) I_i(E) \quad (5)$$

where $n_i(t)$ is the approximation of $n(E, t)$ in the i -th grid interval and N is the number of intervals. $I_i(E)$ is a discrete interval indicator function and defined as [7]:

$$I_i(E) = \begin{cases} 1 & \text{if } E \in [E_i, E_{i+1}] \\ 0 & \text{otherwise} \end{cases} \quad (6)$$

Equation (1) is then integrated over the interval $E \in [E_i, E_{i+1}]$. Taking an equidistant energy grid with a small finite increment, so that $\Delta E_i = \Delta E_j = \text{const}$, and setting an upper boundary E_{max} for the theoretically unlimited energy range, results in the conventional discrete form of the ME [7]:

$$\frac{d}{dt} \vec{n}(t) = [\omega(\mathbf{P} - \mathbf{I}) - \mathbf{K}] \vec{n}(t) + R_a \vec{f} \quad (7)$$

or in more compact form:

$$\frac{d}{dt} \vec{n}(t) = \mathbf{J} \vec{n}(t) + R_a \vec{f} \quad (8)$$

Here, \vec{n} is a vector with elements $n_i(t)$, \vec{f} is a vector of nascent distribution of incoming flux of activated reactant molecules $f_i = f(E_i)$, \mathbf{P} is the collision transition probability matrix with elements $P_{ij} = P(E_i, E_j) \Delta E_i \Delta E_j$, \mathbf{I} is the unit matrix and \mathbf{K} is a diagonal matrix with $K_{ii} = k_{\Sigma}(E_i)$.

The quasi-spectral method projects the solution into space of arbitrarily placed GRBFs over entire energy range. Thus the solution is derived in form of weights of basis functions. The exact solution of the ME, $n(E, t)$ can be approximated with a weighted sum of N basis function $\varphi_j(E)$ [8]:

$$n(E, t) \approx \sum_{i=1}^N n_i(t) \varphi_i(E) \quad (9)$$

where $n_i(t)$ are the time-dependent spectral coefficients. To identify the unknown weights $n_i(t)$, the Ritz-Galerkin

method can be used [8], i.e. eq. (9) is substituted into eq. (1) and both sides of the equation are multiplied by a test function $\varphi_i(E)$ and then integrated over the interval $E \in [0, +\infty]$:

$$\begin{aligned} & \sum_{j=1}^N \frac{dn_j(t)}{dt} \cdot \int_E \varphi_j(E) \varphi_i(E) dE \\ &= \int_E R_a f(E) \varphi_i(E) dE \\ &+ \omega \sum_{j=1}^N n_j(t) \int_{E'} \varphi_j(E') \int_E P(E, E') \varphi_i(E) dE dE' \\ &- \omega \sum_{j=1}^N n_j(t) \int_E \varphi_j(E) \varphi_i(E) dE \\ &- \sum_{j=1}^N n_j(t) \int_E k_{\Sigma}(E) \varphi_j(E) \varphi_i(E) dE, \end{aligned} \quad (10)$$

where $i = 1, 2, \dots, N$. The formula (10) can also be written in vector-matrix form like equation (7):

$$\mathbf{A} \frac{d}{dt} \vec{n}(t) = [\omega(\mathbf{P} - \mathbf{A}) - \mathbf{K}] \vec{n}(t) + R_a \vec{f} \quad (11)$$

where \vec{n} is the vector of unknowns, \mathbf{A} , \mathbf{P} and \mathbf{K} are matrices and \vec{f} is a vector:

$$\mathbf{A}_{ij} = \int_E \varphi_j(E) \varphi_i(E) dE \quad (12a)$$

$$\mathbf{P}_{ij} = \int_{E'} \varphi_j(E') \int_E P(E, E') \varphi_i(E) dE dE' \quad (12b)$$

$$\mathbf{K}_{ij} = \int_E k_{\Sigma}(E) \varphi_j(E) \varphi_i(E) dE \quad (12c)$$

$$\underline{f}_i = \int_E f(E) \varphi_i(E) dE \quad (12d)$$

Comparing formula (7) with (11), it is apparent that both linearised vector-matrix forms of the ME are formally very similar. Moreover, if the basis functions $\varphi_i(E)$ in the formula (9) are defined as the discrete interval indicator function $I_i(E)$, equation (11) reduces to the conventional form (7).

Gaussian radial basis functions (GRBF) are particularly promising because of their algebraic simplicity and opportunities for combining spectral accuracy with local refinement [9]. GRBFs have a similar exponential form to the equilibrium energy-dependent population and reflects the features of the probability of collisional energy transferred. Furthermore using the normalization the shape of GRBFs is automatically adjusted to the irregular grid, that determines the location of the function centers on the energy scale. In this work the following normalized form of the

GRBFs is applied:

$$\varphi_i(x) = \frac{\exp\left[-\frac{(x-x_i)^2}{\sigma_i^2}\right]}{\sum_j \exp\left[-\frac{(x-x_j)^2}{\sigma_j^2}\right]} \quad (13)$$

Here σ_i is the width factor of the GRBF. A larger σ corresponds to a wider basis function and a smaller σ corresponds to a narrower one. The width factor is chosen for each GRBF such that the function $\varphi_i(x)$ crosses its neighbours (φ_{i-1} and φ_{i+1}) near the half maximum of the function.

The observable individual rate coefficient for the l -th reaction channel is obtained from the relation [1–3]:

$$k_l(T, p) = \frac{\int_0^{+\infty} n(E, t \rightarrow \infty) k_l(E) dE}{\int_0^{+\infty} n(E, t \rightarrow \infty) dE} \quad (14)$$

Because the systems (7) and (11) are linear, the general time-dependent solution for thermal activation ($R_a = 0$) is [1–4]:

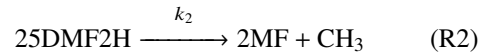
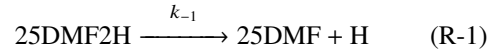
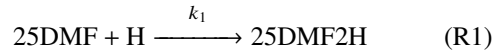
$$\vec{n}(t) = \sum_{i=0}^N e_i \exp(\lambda_i t) \vec{v}_i \quad (15)$$

Here λ_i are the eigenvalues of J and \vec{v}_i are the conjugated and linearly independent eigenvectors. e_i are the expansion coefficients determined from the initial conditions. All eigenvalues λ_i are negative and it is often the case that the first eigenvalue is well separated from the others $|\lambda_0| \ll |\lambda_1| < \dots < |\lambda_N|$ [1–3]. In this case, the evolution of \vec{n} can be described by a mono-exponential decay after an induction period in the order of $1/|\lambda_1|$. Although after this period, the integrated population decreases continuously, the normalized distribution remains unchanged. In this work the normalized distribution corresponding to mono-exponential decay is considered as the long-time distribution for the thermally activated ME. If the separation of eigenvalues is not given (e.g. high temperature), care must be taken when interpreting the result in the way described above. However, this should have no impact on the numerical comparison between the conventional method and the QSM.

Example system: Decomposition of 25DMF2H

As a case study for the comparison of the QSM with the CDM, the decomposition of 25DMF2H was chosen. It is an important intermediate radical in the pyrolysis and combustion of 2,5-dimethylfuran (25DMF). 25DMF is a potential biofuel, which has many positive features such as: the energy density comparable with gasoline, high boiling point, high octane number, etc [10]. The reactions of 25DMF2H were investigated experimentally by Friese et al. [11], intensively studied by Somers et al. [10] and Sirjean et al [12]. This radical is formed at first via addition of an H atom to the carbon in α -position to the oxygen in 25DMF. The product (25DMF2H) can either

decompose back to the reactants via C-H fission (R-1) or undergo a C-C bond scission to form a methyl radical and 2-methylfuran (2MF):



The thermal unimolecular reactions (R-1) and (R2) are considered in the ME without incoming flux. The formation reaction (R1) is considered additionally for the ME with incoming flux, since this step causes the nascent chemical activation of 25DMF2H. The threshold energies for both reactions were adopted from [11], rotational constants and unscaled vibrational frequencies of the reactant and transition states were obtained from [13].

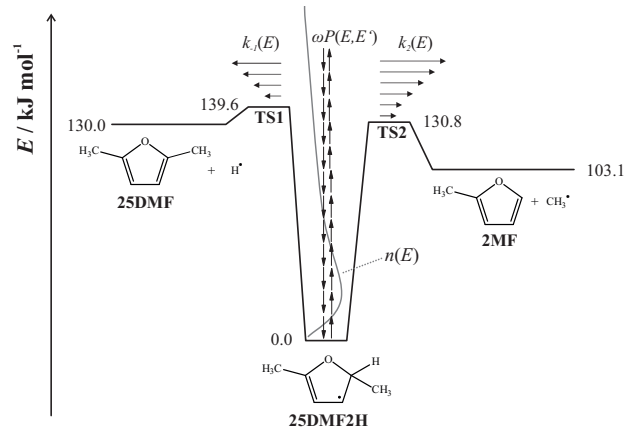


Figure 1: Schematic representation of the potential energy diagram describing the unimolecular decomposition of 25DMF2H

For the collisional energy transfer probability, a modified empirical exponential down model introduced by Eng et al. [14] is used:

$$P(E, E') = \frac{1}{N(E')} \exp\left[-\left(\frac{E'-E}{\alpha}\right)\right] \rho(E) \rho(E') \quad \forall E < E' \quad (16)$$

Here $N(E')$ is the normalization constant to satisfy the principle of completeness and α is a parameter which determines the average energy transferred per collision.

For α in $P(E, E')$, a value of 250 cm^{-1} was assumed on the basis of the parameter ΔE_{SL} used in [11]. The latter is part of the step-ladder model for $P(E, E')$ and it is related to α in the exponential-down model. The Lennard-Jones parameters of 25DMF as a proxy for 25DMF2H were taken from [11] and the collision partner molecules are argon (Ar), which yields the averaged Lennard-Jones parameters $\epsilon_{25\text{DMF2H-Ar}}/k_B = 239 \text{ K}$ and $\sigma_{25\text{DMF2H-Ar}} = 4.4 \text{ \AA}$. The specific rate constants $k(E)$ were calculated from RRKM theory [1–4] for an angular momentum quantum number $J=110$, which is the thermal average for 25DMF2H in the temperature range between 950 and 1250K. As in [11], the J dependence of $k(E)$ for the tight transition states was assumed to be weak.

As no analytic solution is known for the current example, the conventional method with $\Delta E = 10 \text{ cm}^{-1}$ (see [7] for the validation) is chosen as a reference. The effectiveness (computational time, accuracy etc.) of the QSM and the CDM is compared using two measures: relative error and relative computational (CPU) time. The relative error is defined as:

$$\epsilon(p, T) = \left| \frac{k_{ref}(p, T) - k(p, T)}{k_{ref}(p, T)} \right| \quad (17)$$

Here $k_{ref}(p, T)$ means the rate constants at pressure p and temperature T calculated by the reference method and $k(p, T)$ is the approximate rate constant calculated with a smaller linear system size, using either the CDM or the QSM.

The relative (normalized) CPU time is:

$$\tau = \frac{t}{t_{ref}}, \quad (18)$$

where t_{ref} is the CPU time of the reference method, t is the actual CPU time of the studied method.

The most important feature that affects the effectiveness of a method is the size of the corresponding linear system. i.e. the number of grid points for the discretized linear form of the ME (7) and the number of basis functions for the QSM (11).

Results and Discussion

The results of the proposed quasi-spectral method (QSM) have been compared with the conventional method (CDM) for the range of typical combustion temperatures from 800 to 2000 K and pressures from 10^{-8} to 100 bar. The range of temperatures and pressures was extended beyond the experimentally available data to evaluate the robustness of the suggested method. The pressure range was formally chosen to cover a broad spectrum of collision frequencies between 20 and 10^{11} s^{-1} including experimental conditions that may occur in the investigation of elementary reactions in combustion. An equilibrium distribution at given temperature was taken as the initial distribution for all numerical tests. A typical solution (normalized distribution corresponding to the mono-exponential decay) is shown in Fig. 2.

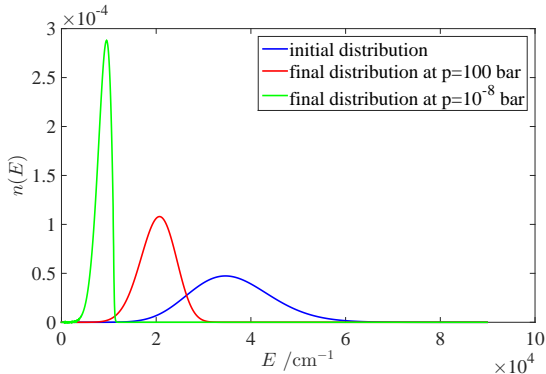


Figure 2: Normalized Initial and final distributions at T=2000 K

Fig. 3 and Fig. 4 show the convergence of the conventional and the proposed methods. The QSM has an apparently faster convergence rate for all studied temperature and pressure ranges. This method was particularly advantageous for high pressures. As it is shown in Fig. 2, the final population distribution tends to the equilibrium distribution and is very similar to the applied GRBF. In the low pressure limit, the end distributions requires a larger number of basis functions to approximate. In general the ME can be described with QSM using at least 10 times less system parameters than using the CDM (for errors below 0.5%). This information is presented in a compact form in Fig. 5 and Fig. 6, which show the relative errors for different combination of temperature and pressure with the fixed system size. The CDM can achieve overall accuracy below 0.5% if at least 2000 grid points are used (see. Fig. 5). This error varies very little across the studied p-T domain (see Fig. 5). The QSM can achieve the same accuracy with only 200 basis functions but most part of the p-T domain is covered with an error well below 0.1%.

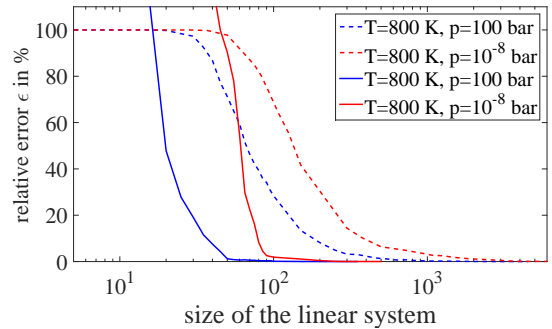


Figure 3: Relative errors vs. system size at T=800 K. Dashed - CDM; Solid - QSM

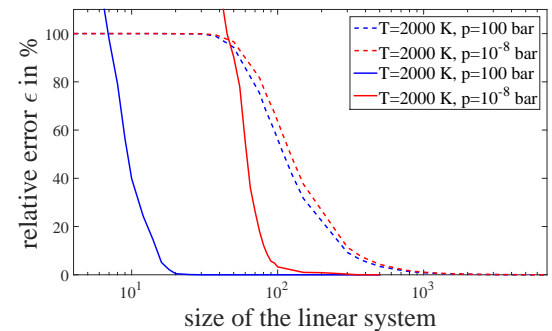


Figure 4: Relative errors vs. system size at T=2000 K. Dashed - CDM; Solid - QSM

The obvious advantage of the reduced size of the linear system is the lower computational time. Figs. 8, 9 illustrate the correlation of the relative error and the minimal computational time required to achieve this accuracy with different system sizes. If 0.5% relative errors must be achieved, at T=800 K the QSM is at least 5 times faster than the CDM for all pressures; at T=2000 K – twice as fast at the highest studied pressure and eight times faster at the lowest studied pressure. The computational speed-up for a relative error of 0.5% at high temperature and high pressure (T=2000 K and p=100 bar) is not so obvious since

in this limit, the energy-dependent distribution is so wide that a fine discretization is not necessary and indeed, as shown in Fig.4, only approx. 500 grid points are sufficient. However, if a relative error below 0.2% at T=2000 K and p=100 bar is desired, the QSM has again a clear advantage and is more than 5 times faster than the conventional method.

Although the linear system size of the QSM is at least 10 times smaller than that of the conventional method, the achieved net speed-up is about 5 to 8 times. The attenuation of the performance advantage arises from the computation of the spectral equivalent of the collision transition probability matrix (12b). However, for the study of a pressure dependence of the rate coefficient (14), this matrix is kept unchanged, which gives a tremendous implicit speed-up, if it is calculated only once and then reused for different pressures at the same temperature.

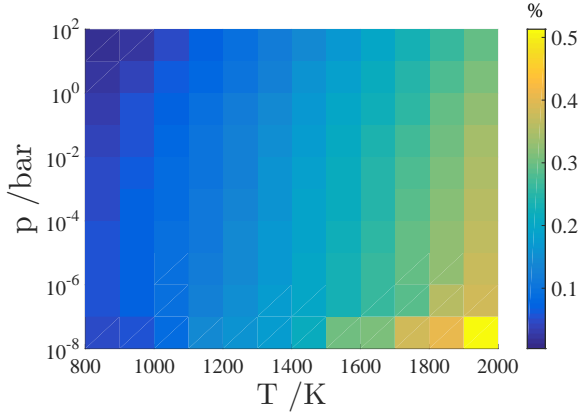


Figure 5: Relative error of the CDM for the temperature range from 800 to 2000 K at the pressure range from 10^{-8} to 100 bar with system size $N=2000$

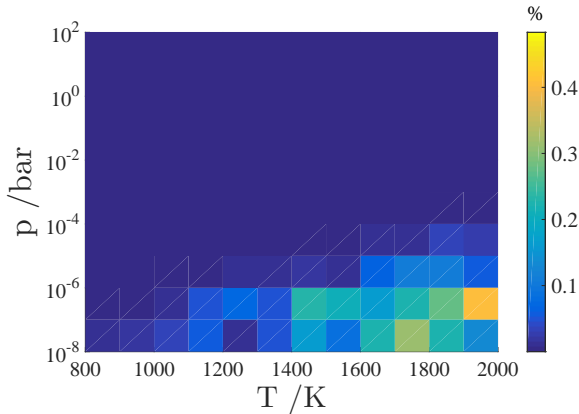


Figure 6: Relative error of the QSM with equidistant grid for the temperature range from 800 to 2000 K at the pressure range from 10^{-8} to 100 bar with system size $N=200$

As shown in [7] the location of the energy maximum according to the end distribution can still provide a good approximation of the end distribution for the cost of the accurate time-dependent solution. Mathematically it can be seen as applying the reverse Heaviside step function as a grid density function (GDF). Observing that most

changes occur near the reaction channel, a reverse sigmoid function, placed at the threshold energy of k_{Σ} (2), provides a far better approximation without the loss of accuracy of the transient population evolution at short timescales:

$$G(E) = 1 - \frac{1}{1 + e^{-(E-E_{threshold})/\sigma}} \quad (19)$$

$G(E)$ is the grid density function and σ is a bend smoothness factor. This factor can be determined using an approximated solution (e.g. one with a very crude regular grid). Fig. 7 shows the distribution of 20 GRBFs according to the inverse sigmoid function with parameter $\sigma = 4500 \text{ cm}^{-1}$, which is optimal for the given example at T = 1100 K and p = 0.01 bar.

Fig. 10 presents an error map for 40 non-equidistantly placed GRBFs with sigmoid grid density function for the entire p-T study domain. Again half of the domain (lower temperatures and higher pressures) can be approximated with a far better accuracy than 0.1% and the relative error of 0.5% is guaranteed in the entire domain.

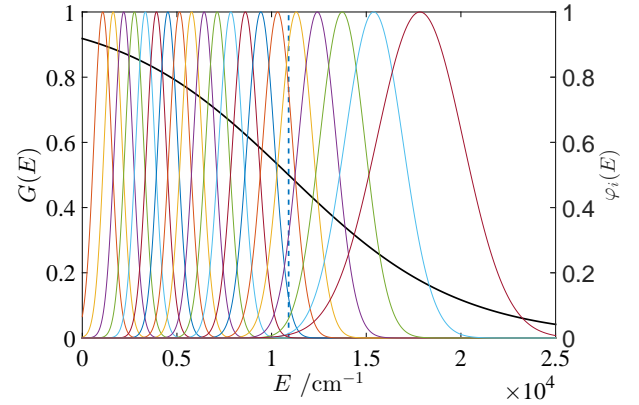


Figure 7: Example GRBF distribution with grid density function. Solid black line - GDF, Dashed blue line - Energy threshold

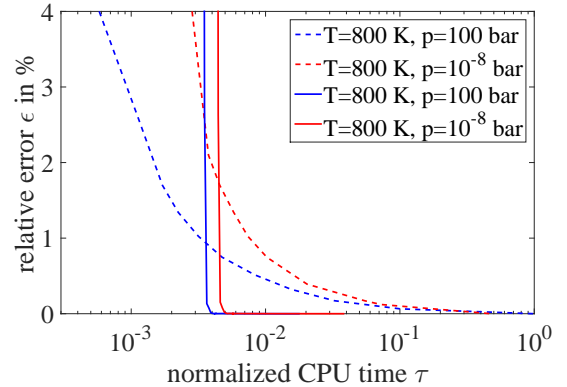


Figure 8: Accuracy over calculation time at T=800 K. Dashed - CDM; Solid - QSM

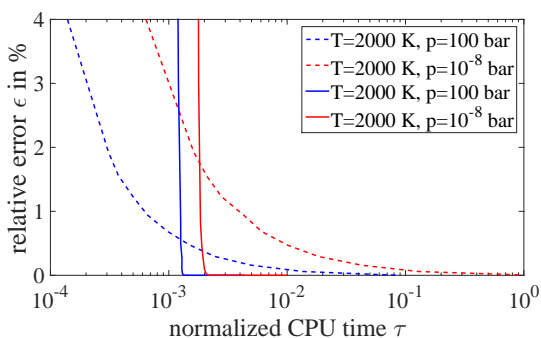


Figure 9: Accuracy of different methods over calculation time at $T=2000$ K. Dashed - CDM; Solid - QSM

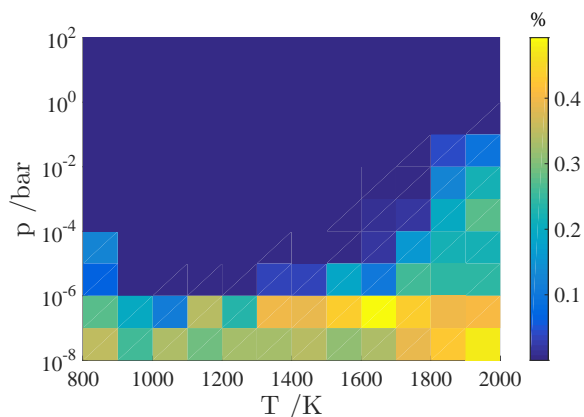


Figure 10: Relative error of the QSM with non-equidistant grid for the temperature range from 800 to 2000 K at the pressure range from 10^{-8} to 100 bar with system size $N=40$

Conclusions

The computational efficiency of the conventional discretization method for solving the continuum master equation may limit its further application (e.g. in studies of systems of coupled MEs). In this work an investigation has been made on reducing of the system dimensionality and thus increasing the efficiency.

The proposed quasi-spectral method employs the smoothness and specific bell-like shape of the reactant distribution by projecting the solution into a space of Gaussian radial basis functions (GRBFs). Equidistantly located GRBFs can reduce the system size at least by a factor of 10 compared to the CDM without losing accuracy with corresponding speed-up of 5 to 8 times. This speed-up can even be enhanced, when several calculations at constant T and variable P are combined to a single pass, thus avoiding the costly recalculation of the P matrix for each (T, P) pair.

If an irregular grid of GRBFs is applied, the resulting system is by a factor of 50 smaller than an equivalent conventional system. The proposed method uses the inverse sigmoid function as a grid density function, whose parameters are determined from a crude first approximation of the solution.

The empirical studies indicate that the performance of the method for a single ME can be improved using an irregular grid but the computational advantage compared with the equidistant grid remains within the same order of magnitude. However, in a case of several coupled MEs

with multiple reaction pathways, when the system size increases dramatically, the speed-up should be more pronounced. An optimal grid for coupled MEs is the subject of ongoing research.

References

- [1] R. Gilbert, S. Smith, Theory of Unimolecular and Recombination Reactions, Physical chemistry texts, Blackwell Scientific Publications, 1990.
- [2] K. A. Holbrook, M. J. Pilling, S. H. Robertson, Unimolecular reactions, Wiley New York, 1996.
- [3] W. Forst, Theory of unimolecular reactions, Elsevier, 2012.
- [4] M. Olzmann, Statistical rate theory in combustion: An operational approach, in: F. Battin-Leclerc, J. Simmie, E. Blurock (Eds.), Cleaner Combustion: Developing Detailed Chemical Kinetic Models, Springer: London, UK, 2013, pp. 549–576.
- [5] M. Pfeifle, M. Olzmann, Consecutive chemical activation steps in the oh-initiated atmospheric degradation of isoprene: An analysis with coupled master equations, International Journal of Chemical Kinetics 46 (4) (2014) 231–244.
- [6] M. P. Burke, C. F. Goldsmith, Y. Georgievskii, S. J. Klippenstein, Towards a quantitative understanding of the role of non-boltzmann reactant distributions in low temperature oxidation, Proceedings of the Combustion Institute 35 (1) (2015) 205–213.
- [7] A. Koksharov, M. Pfeifle, V. Bykov, et al., On the numerical solution of the chemical master equation, Proceedings of the European Combustion Meeting 2013.
- [8] J. P. Boyd, Chebyshev and Fourier spectral methods, Courier Dover Publications, 2001.
- [9] B. Fornberg, C. Piret, On choosing a radial basis function and a shape parameter when solving a convective {PDE} on a sphere, Journal of Computational Physics 227 (5) (2008) 2758 – 2780.
- [10] K. P. Somers, J. M. Simmie, F. Gillespie, et al., A high temperature and atmospheric pressure experimental and detailed chemical kinetic modelling study of 2-methyl furan oxidation, Proceedings of the Combustion Institute 34 (1) (2013) 225–232.
- [11] P. Friese, J. M. Simmie, M. Olzmann, The reaction of 2, 5-dimethylfuran with hydrogen atoms—an experimental and theoretical study, Proceedings of the Combustion Institute 34 (1) (2013) 233–239.
- [12] B. Sirjean, R. Fournet, Theoretical study of the reaction 2, 5-dimethylfuran+ h products, Proceedings of the Combustion Institute 34 (1) (2013) 241–249.
- [13] J. M. Simmie, W. K. Metcalfe, Ab initio study of the decomposition of 2, 5-dimethylfuran, The Journal of Physical Chemistry A 115 (32) (2011) 8877–8888.
- [14] R. A. Eng, A. Gebert, E. Goos, H. Hippler, C. Kachi-ani, Branching ratios and incubation times in the thermal decomposition of methyl radicals: Experiments and theory, Physical Chemistry Chemical Physics 3 (12) (2001) 2258–2267.